Journal of Applied Polymer Science

# High temperature shape memory polyimide ionomer

**Yongkang Bai,[1] Long Mao,[1] Yuejun Liu[1,2]**

[1]School of Materials Science and Engineering, Xiamen University of Technology, 600 Ligong Road, Xiamen, People's Republic of China

[2]Key Laboratory of New Materials and Technology for Packaging, College of Packaging and Materials Engineering, Hunan University of Technology, 88 Taishan Road, Zhuzhou, People's Republic of China

Correspondence to: Y. Bai (E-mail: yongkangbai@sina.com) and Y. Liu (E-mail: yjliu_2005@126.com)

**ABSTRACT:** In this work, a high temperature shape memory polymer based on polyimide (PI) ionomer is prepared by introducing ionic crosslinked interaction. The ionic crosslinked points are introduced to polymer networks through the reaction between polyamic acid and calcium hydroxide before thermal imidization. The crosslinked reaction, microtopography, mechanical, thermal, and shape memory properties of PI ionomers are systematically investigated. The results show the introduction of ionic crosslinked interaction could enhance the glass transition temperature, mechanical, and shape recovery performance of ODA-ODPA, a PI. The prepared ionomers exhibit good high temperature shape memory properties around 270 °C. The shape fixation and shape recovery ratio are over 99% and 90%, respectively. This method provided a new sight of preparing high temperature shape memory polymer, which could be used in severe conditions, like aerospace industry field. © 2016 Wiley Periodicals, Inc. J. Appl. Polym. Sci. **2016**, *133*, 43630.

**KEYWORDS:** functionalization of polymers; polyimides; properties and characterization; stimuli-sensitive polymers

Received 10 December 2015; accepted 13 March 2016

**DOI: 10.1002/app.43630**

## INTRODUCTION

Shape memory polymers (SMPs) are a kind of smart materials which can memorize their original shape.[1,2] They are capable of recovering to the presupposed shape from a temporary shape upon exposing to external stimuli, such as thermal, solvent, light, or pH.[3,4] With this attractive property, SMP has great potential in biomedical and surgical materials, smart fabrics, aerospace industry, temperature sensors, and actuators.[5–7]

During the past decades, many polymers have been adopted to prepare SMPs, such as polyolefines,[8] polystyrene,[9] polysiloxane,[10] poly(methyl-acrylates),[11] polycaprolactone,[12] and DNA.[13] To realize shape memory effect, polymers need to fulfill suitable molecular networks architecture, which consists of two aspects: reversible phase and fixed phase.[14,15] The reversible phase can be crystalline or amorphous phase, which is sensitive to particular external stimuli and capable of fixing the temporary shape. The fixed phase, or called netpoints, can be chemically or physically crosslinked points, which is response for memorizing the original shape. For example, Voit's group[16] prepared chemically crosslinked polymer networks based on methyl acrylate and isobornyl acrylate, which showed excellent shape memory effect with recoverable strains over 800%. Lourdin's group[17] used starch to prepare a bio-SMP based on hydrogen-bond interaction as fixed phase. Besides, a novel polymer networks crosslinked by metal ions catches researchers' attention recently. For example, Weiss[18] reported a high temperature shape memory poly(ether ether ketone) ionomer with metal ionic networks as fixed phase. The ionic crosslinked interactions between metal group sulfonate groups provide the crosslinked points endowing the ionomers with high shape memory properties.

Aromatic polyimide (PI) is a kind of high performance engineering material with high glass transition temperature ($T_g$), high thermal stability, high mechanical strength and excellent radiation shielding capability. The usage of PI as high temperature SMP could widen the potential application in severe conditions undergo high temperature, like deploy space structure, smart jet propulsion system, high temperature sensors and actuators.[19,20] In our previous study, we have found that ODA-BPDA, a PI, with high chain rigidity and linearity could show well shape memory properties due to strong π-π interaction.[21] But for ODA-ODPA with weak π-π interaction, it showed poor shape memory properties with shape recovery ratio less than 55%. Then, we wonder whether some simple method can be adopted to improve the shape recover ratio of ODA-ODPA. According to previous studies, two methods have been used to

Additional Supporting Information may be found in the online version of this article.

enhance the shape memory properties of PI. Yoonessi[22] prepared PI nanocomposites filled with graphene and graphene derivatives. They found the shape recovery performance of PI could be improved with the addition of graphene materials due to the increase of π-π interaction. Vaia[23] and Jinsong Leng[24] improved the shape memory properties by preparing thermoset polyimide with chemically crosslinked points.

In this study, the ionic crosslinked method was used to improve the shape memory properties of PI. It is known that PI is usually prepared by a two-step method: synthesis of polyamic acid (PAA) and imidization. Therein, PAA is a kind of polybasic acid which could be converted to polyamic acid salt by reacting with metal hydroxide. Herein, we introduced the ionic crosslinked points by reacting PAA with calcium hydroxide before thermal imidization. The ionic crosslinked interaction could be introduced to PI, but at the meantime the molecular structure of PI would be destroyed. These two effects may exert opposite influence on properties of PI. So two kind of PI (ODA-ODPA and ODA-BPDA) were used to prepare PI ionomers to study the improvement of shape memory properties. In addition, the influence of ionic crosslinked interaction on the microtopography, thermal, mechanical of PI were carefully investigated and discussed.

## EXPERIMENTAL

### Materials

3,3′,4,4′-biphenyltetracarboxylic dianhydride (BPDA) was supplied by Changzhou Sunlight Pharmaceuticl Co., Ltd. 4.4′-oxydiphthalic dianhydride (ODPA) was obtained from Shanghai Research Institute of Synthetic Resin. 4,4′-Oxydianiline (ODA) and calcium hydroxide ($Ca(OH)_2$) was purchased from Sinopharm Group Chemical Reagent Co., Ltd. The average grain diameter of $Ca(OH)_2$ was about 44 μm. *N*-methyl-2-pyrrolidone (NMP) was received from Shanghai Kefeng Industry & Commerce Co., Ltd.

### Preparation of Polyimide

The synthesis of polyimide (PI) was conducted according to previous studies.[25,26] In brief, 0.01 mol of ODA was first dissolved in 50 mL of NMP at a three-necked flask and stirred under dry nitrogen for 30 min. Then 0.01 mol of ODPA or BPDA was slowly added to the flask in batches within 20 min and intense mechanical stirring was executed for 24 h to afford a polyamic acid (PAA) solution. Finally, the PAA solution was poured on glass support and a stepwise thermal imidization was carried out at 70 °C/4 h, 100 °C/1 h, 200 °C/1 h, 300 °C/1 h to obtain a PI film.

### Preparation of Polyimide Ionomer

To synthesize PI ionomer, the PAA solution was also prepared first and then a certain amount of $Ca(OH)_2$ (0.1 mmol, 0.5 mmol, and 1 mmol) was added. The mixture was stirred for another 120 h until the turbid solution was completely clarified to ensure the complete reaction between $Ca(OH)_2$ and carboxyl groups. Finally, the PAA ionomer solution was also cast onto a glass plate and underwent the same imidization curing process with PI. The schematic illustration for the process was shown in Figure 1.

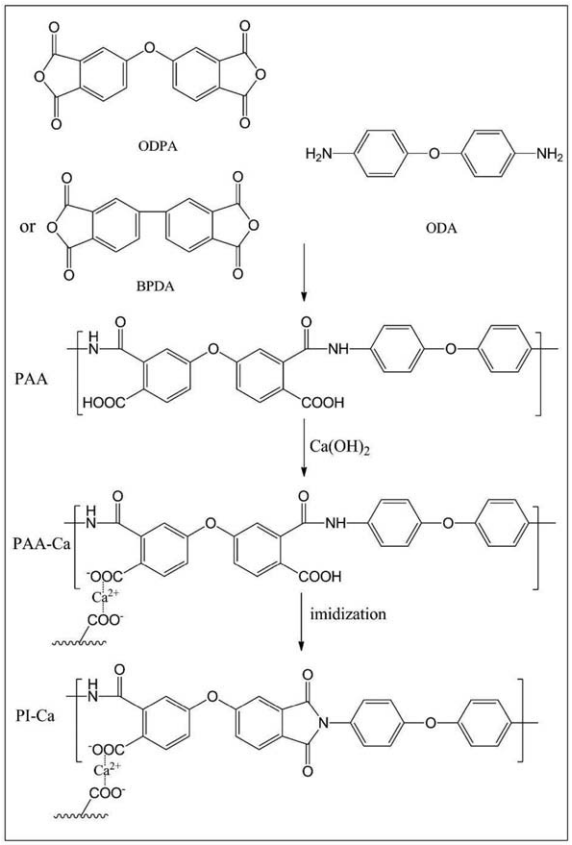


**Figure 1.** Schematic of synthesis of PI ionomer with ODPA and ODA as example.

### Materials Characterization

Fourier transform infrared spectroscopy (FTIR) spectra were obtained by Nicolet 380 IR spectrophotometer with a spectral range of 400–4000 $cm^{-1}$. X-ray photoelectron spectroscopy (XPS) was conducted on a PHI-5702 electron spectrometer (Perkin-Elmer) using an AlKa line excitation source. The fractured surfaces of PI ionomers were measured using a field emission scanning electron microscope (FESEM, JSM-6710F). All samples were coated with gold by sputtering before analyzing. The mechanical properties of PI and ionomers were investigated by a universal testing machine (Shimadzu AG-X) with a strain speed of 5 mm $min^{-1}$ at room temperature. The tested samples were cut to dog-bone type dimension according ISO527-2/1BB.

The dynamic thermomechanical properties of the specimens were characterized by dynamica mechanical analysis (DMA) on Netzsch DMA 242C. DMA tests were performed in tensile mode at the frequency of 1 Hz with a heating rate of 5 °C $min^{-1}$ from 25 °C to 400 °C. The samples were cut into dimensions of ~20 × 3 × 0.05 $mm^3$. Thermogravimetric analysis (TGA) was carried out under nitrogen atmosphere on LABSYS evo TGA/STA using a heating rate of 10 °C $min^{-1}$ from 25 °C to 800 °C.

The shape memory properties were measured from shape memory cycles carried out by DMA 242C under tensile mode. The procedure for cyclic tensile tests contains the following steps: (a) heating a sample (with origin strain of $\varepsilon_A$) to $T_g + 50$ °C

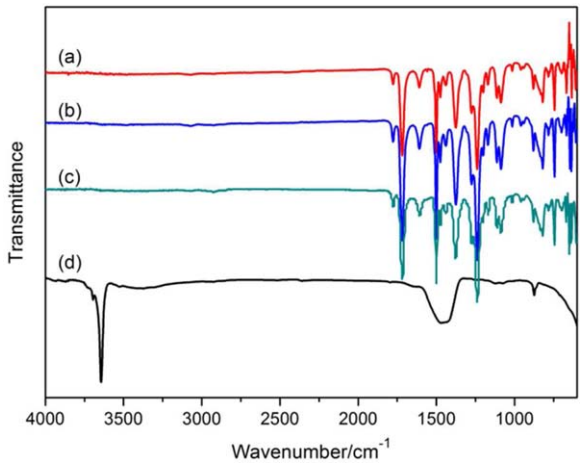


**Figure 2.** FTIR spectra of (a) ODA-ODPA-1, (b) ODA-ODPA-5, (c) ODA-ODPA-10, and (d) $Ca(OH)_2$. [Color figure can be viewed in the online issue, which is available at wileyonlinelibrary.com.]

under a constant force, (b) reducing the temperature to a low temperature (20 °C) leading to a strain of $\varepsilon_{B,load}$, (c) remove the force to afford the temporary strain of $\varepsilon_B$, (d) reheating to $T_g + 50$ °C again to afford the recovery strain $\varepsilon_{A.rec}$. The heating and cooling rates during the procedure were both 5 °C $min^{-1}$. The shape memory properties were evaluated by shape fixation ($R_f$) and shape recovery ratio ($R_r$) calculated by eqs. (1) and (2). Wherein, $R_f$ represented the capability of fixing the temporary shape, while $R_r$ represented the capability of memorizing the original shape. $\varepsilon_x$ represented the strain of each shape taken from the strain curve.

$$R_f = (\epsilon_B - \epsilon_A)/(\epsilon_{B,\ load} - \epsilon_A) \quad (1)$$

$$R_r = (\epsilon_B - \epsilon_{A,\ rec})/(\epsilon_B - \epsilon_A) \quad (2)$$

## RESULTS AND DISCUSSION

In this study, two PIs are adopted to prepare PI ionomers with different crosslinked degree, which are named as ODA-ODPA-*n* and ODA-BPDA-*n*, respectively (*n* represented the mole percentage of $Ca(OH)_2$ to monomer). The ionic crosslinked reaction is based on the acid-base reaction between $Ca(OH)_2$ and carboxy group, as shown in Figure 1. The crosslinked reaction could be confirmed first by the change of turbidity of reaction liquid. In the Supporting Information Figure S1, it is obvious that reaction liquid became turbid after the addition of $Ca(OH)_2$. After reacting 5 days, the reaction liquid turned to clarified, meaning the complete reaction of $Ca(OH)_2$. Furthermore, FTIR spectra is used to confirmed the complete reaction of $Ca(OH)_2$ with PAA. As observed in Figure 2, taking ODA-ODPA as example, the strong absorption peak at 3644 $cm^{-1}$ on (d) curve is ascribed to the stretching vibration of free $OH^-$ on $Ca(OH)_2$. This peak disappears from the spectra of ionomers (a to c), indicating the complete reaction of $Ca(OH)_2$. In order further confirm the formation of Ca and PI, another characterization method XPS is added (as shown in Supporting Information Figure S2). The results show that the binding energy of Ca2p in $Ca(OH)_2$ is about 346.9 eV, while it is 344.4 eV in ionomer. The decrease of binding energy is ascribed to the decrease of electronegativity from -OH to –OCOR,[27,28] which can prove the existence of ionic crosslinked interaction in ionomers. What's more, the solubility of ionomers is tested. As being a thermoplastics polymer, ODA-ODPA could be dissolved in NMP. But after reacting with $Ca(OH)_2$, the ODA-ODPA-5 and ODA-ODPA-10 are insoluble in NMP, which also can prove the existence of ionic crosslinked interaction in ionomers.

To further confirm crosslinked interaction of $Ca^{2+}$ in ionomers, the fracture surface morphology of PI and ionomers are investigated by SEM, as shown in Figure 3 (taking ODA-ODPA as example). At first, it is clearly found no $Ca(OH)_2$ particle (~44 μm) exists on the fracture surface, indicating that $Ca(OH)_2$ has been reacted absolutely. Besides, PI and ionomers show extremely different fracture surface morphology: the fracture surface of PI is very smooth while ionomers show a rough surface. The fracture surface of ionomers is densely packed with nano-sized bulges and hollows which increase with the increasing content of $Ca^{2+}$. This is attributed to the crosslinked interaction of $Ca^{2+}$. Due to the reinforcement function, the crosslinked points form the concentration of stress during the fracture process, leading to the formation of bulges and hollows.

Then, the mechanical properties were further investigated by a universal testing machine. As presented in Figure 4, the influence of $Ca^{2+}$ on mechanical properties is different to ODA-ODPA and ODA-BPDA. For ODA-BPDA series, the mechanical properties (including tensile strength and elongation at break) decrease obviously with the increase of $Ca^{2+}$. For ODA-ODPA series, the mechanical properties increase first with the increase of $Ca^{2+}$ from 0 to 5%, but decrease when the content of $Ca^{2+}$ reaches 10%. According to previous studies, the high performance of PI mainly comes from its chain structure and intermolecular forces.[26,29] In this study, the introduction of $Ca^{2+}$ as crosslinked points will exert two implications on PI. For one hand, the destructive effect of chain regularity and linearity deteriorate the mechanical properties. It would also weaken the intermolecular forces of PI, especially π-π interaction, which is negative to the mechanical properties. For the other hand, the crosslinked interaction brought by $Ca^{2+}$ can improve the mechanical strength. These two implications will have an antagonistic effect on the mechanical properties. According to their chemical structure, ODA-BPDA possesses higher chain regularity and linearity than ODA-ODPA, so ODA-BPDA has a stronger π-π interaction which has been proved in our previous study.[21] For ODA-BPDA-*n*, the destructive effect plays the major role brought by $Ca^2$, leading to the reduction of its mechanical properties. With a poor chain regularity and linearity, ODA-ODPA possesses weak π-π interaction, so its mechanical strength could be improved by the crosslinked interaction of $Ca^{2+}$.

The crosslinked interaction formed by $Ca^{2+}$ also has great influence on thermal properties of PI, so the dynamic thermomechanical properties are investigated by DMA. The loss factor (tan δ) versus temperature of ODA-ODPA series and ODA-BPDA series is shown in Figure 5(a,b). For ODA-ODPA series, it is obvious that $T_g$ increased with the increase of $Ca^{2+}$ from 260.7 °C of ODA-ODPA to 276.8 °C of ODA-ODPA-10, which

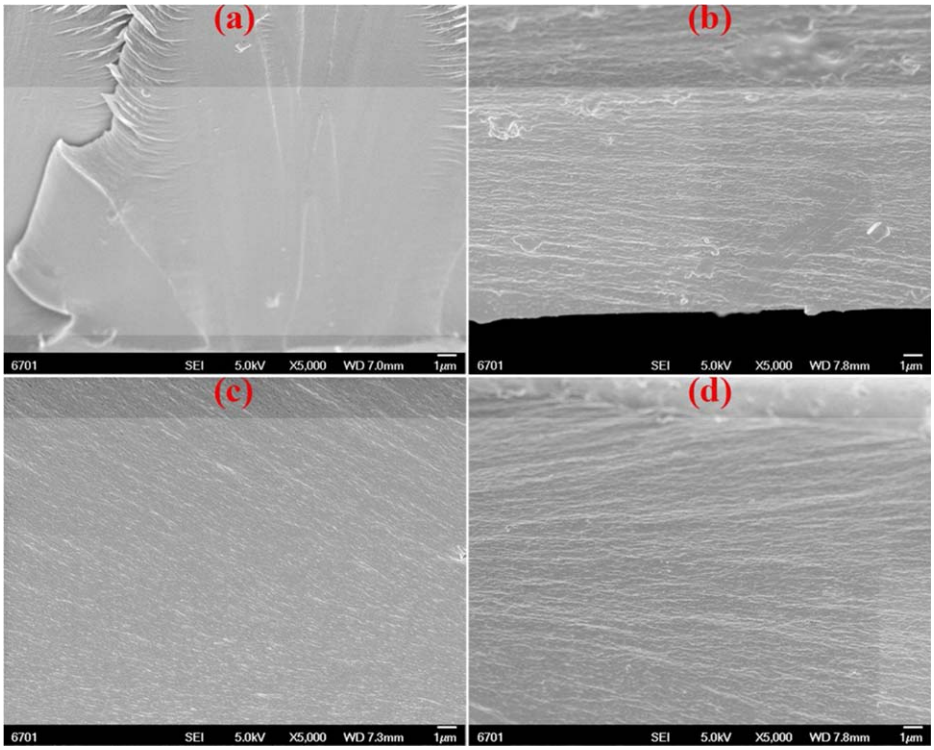


**Figure 3.** The SEM images of fracture surface for (a) ODA-ODPA, (b) ODA-ODPA-1, (c) ODA-ODPA-5, (d) ODA-ODPA-10. [Color figure can be viewed in the online issue, which is available at wileyonlinelibrary.com.]

is mainly attributed to the crosslinked interaction formed by $Ca^{2+}$. But for ODA-BPDA series, the influence of $Ca^{2+}$ on $T_g$ is complicated. With the increase of $Ca^{2+}$, two peaks appear on the tan δ curves. Taking ODA-BPDA-5 as an example, one peak is around 269.6 °C and another is about 286.7 °C. Here, it is deemed that the lower one belongs to thermoplastic part of PI while the higher one is ascribed to the crosslinked interaction of $Ca^{2+}$. It is known that the $T_g$ of polymer is higher with higher chain regularity and linearity.[30] The destructive effect of $Ca^{2+}$ on chain structure will reduce the $T_g$ of ODA-BPDA while the crosslinked interaction produces an opposite effect. Therefore, two peaks appear on the tan δ curves: with the increase of $Ca^{2+}$, the lower one decreases for the destructive effect, while the higher one increases for the crosslinked interaction. Furthermore, Figure 5 presents the storage modulus ($E'$) of PI and ionomers versus temperature. As the curves shown, $E'$ decreases slowly with the increase of temperature at glassy state, then falls dramatically in the vicinity of $T_g$. For example, $E'$ of ODA-ODPA-5 at 200, 260, and 350 °C are 1548.4, 826.7, and 34.8 MPa, respectively. This massive drop of $E'$ is necessary for polymer to realize shape memory effect.[31] As the temperature rises over $T_g$, the sample transforms into rubbery state and then the

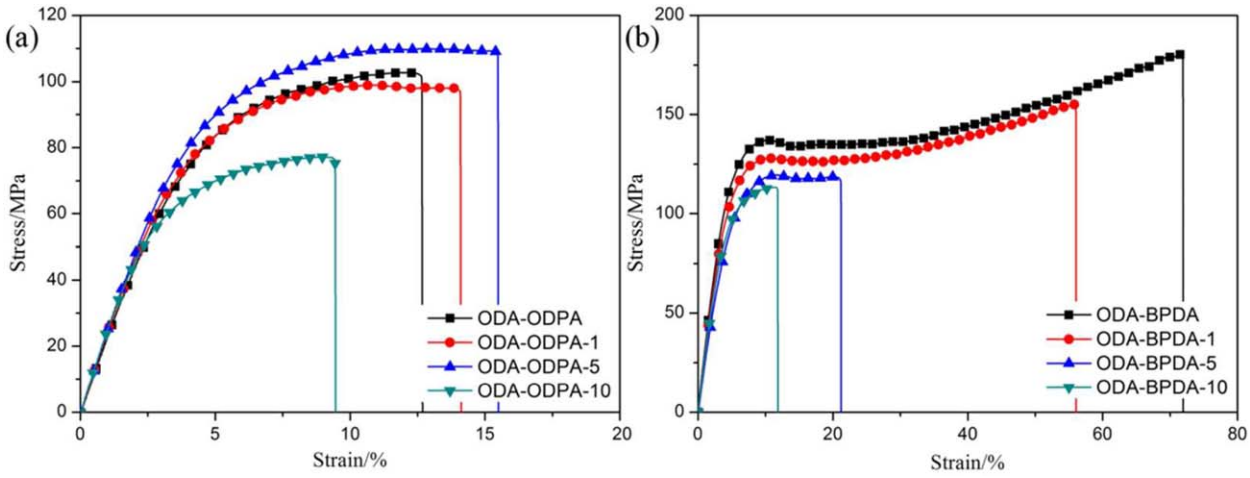


**Figure 4.** Stress-strain curves of (a) ODA-ODPA series and (b) ODA-BPDA series. [Color figure can be viewed in the online issue, which is available at wileyonlinelibrary.com.]

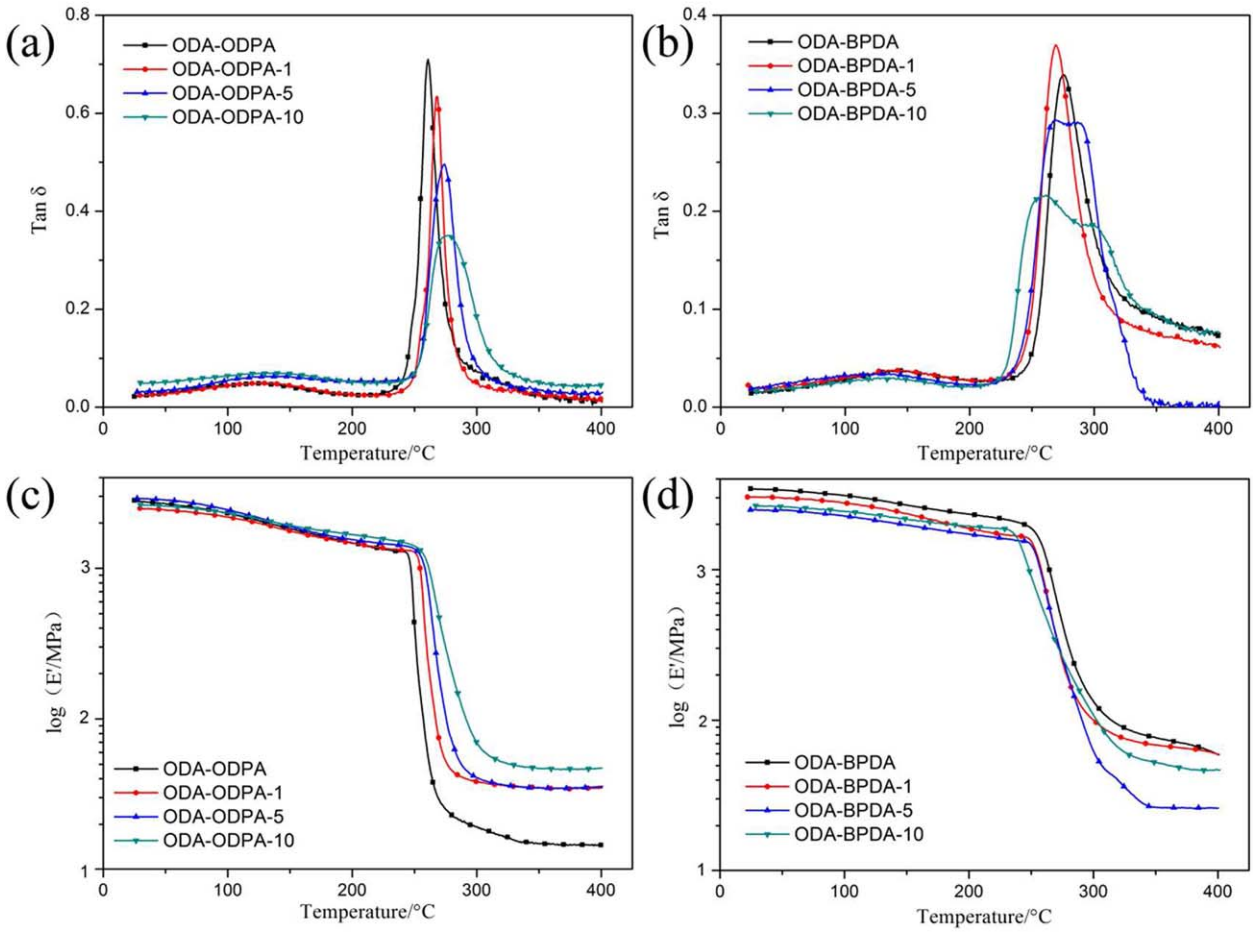


**Figure 5.** Dynamic thermomechanical properties of PI and ionomers: tan δ curves of (a) ODA-ODPA series and (b) ODA-BPDA series; $E'$ curves of (c) ODA-ODPA series and (d) ODA-BPDA series. [Color figure can be viewed in the online issue, which is available at wileyonlinelibrary.com.]

$E'$ keeps the same. Here, it is also presented that the $E'$ of ODA-ODPA series in the rubbery plateau increase with the increase of $Ca^{2+}$ from 15.0 MPa of ODA-ODPA to 46.8 MPa of ODA-ODPA-10, which is due to the increase of crosslinked interaction. The increase of $E'$ at rubbery state for SMP could give rise to a high restoring force when recovery is resisted. But for ODA-BPDA, $E'$ first decreases with the increase of $Ca^{2+}$ from 0 to 5% and then increases when $Ca^{2+}$ reaches 10%. This difference variation tendency is also attributed to the complicated antagonistic effect brought by $Ca^{2+}$ which has been

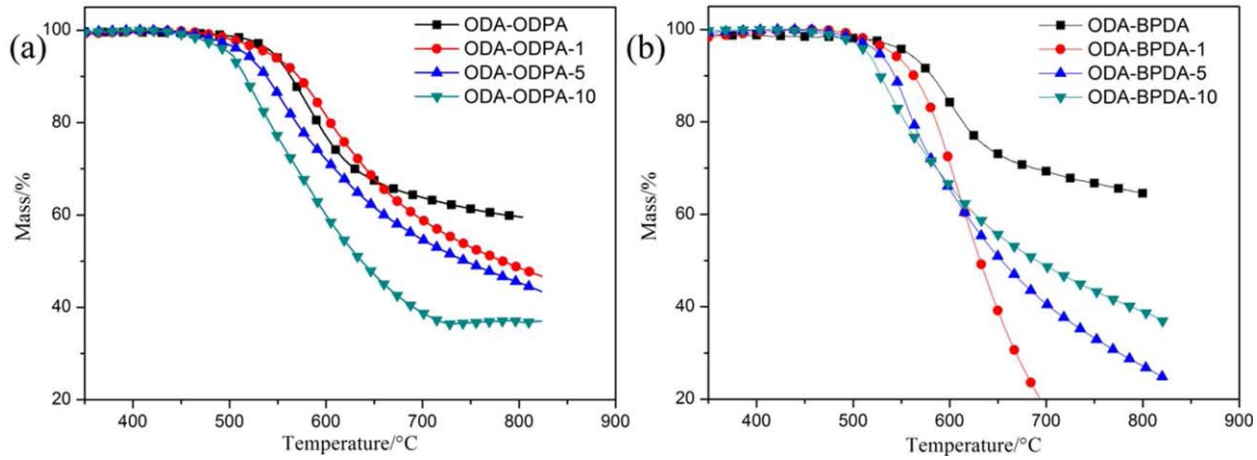


**Figure 6.** TGA curves of (a) ODA-ODPA series and (b) ODA-BPDA series. [Color figure can be viewed in the online issue, which is available at wileyonlinelibrary.com.]

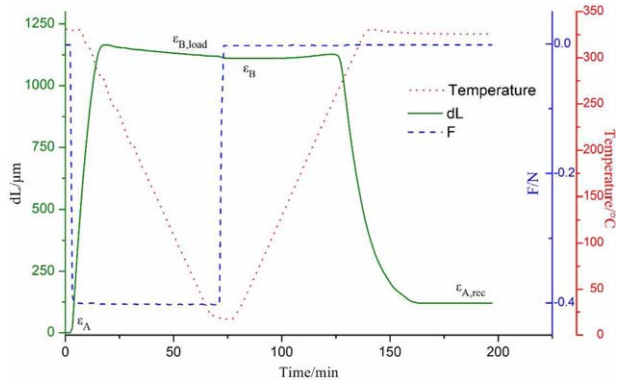


**Figure 7.** A representive shape memory cycle of ODA-ODPA-5. [Color figure can be viewed in the online issue, which is available at wileyonlinelibrary.com.]

discussed above. The thermal stability of PI and ionomers is studied by TGA and the weight loss versus temperature is given in Figure 6. It is clearly that thermal decomposition temperature ($T_{d95}$) of ODA-ODPA and ODA-BPDA both decrease after being crosslinked by $Ca^{2+}$. Considering the influence of $Ca^{2+}$, the destructive effect of chemical structure brought by $Ca^{2+}$ plays the major role among the two implications on the thermo stability of ionomers. Although it decreases due to the introduction of $Ca^{2+}$, the $T_{d95}$ of all ionomers still maintain a high value above 495 °C, indicating the promising application of these materials in engineering field where high service temperature is needed.

According to above investigation, the introduction of $Ca^{2+}$ to PI as crosslinked points will exert difference influence on ODA-ODPA and ODA-BPDA: it could improve the mechanical strength, $T_g$ and $E'$ at rubbery state of ODA-ODPA, but not for ODA-BPDA. So it is still a question whether the introduction of $Ca^{2+}$ could improve the shape memory properties or not. Then the thermal-shape memory properties are investigated using DMA by thermo-mechanical cycles and an example of the fifth shape memory cycle for ODA-ODPA-5 is shown in Figure 7. As shown on the strain curve, the ionomer indeed exhibits good shape memory properties with $R_f$ and $R_r$ about 99.1% and 90.0%, respectively. Figure 8 presents the shape memory properties of PI and inonmers. From the data of Figure 8(a), the $R_f$ of ODA-ODPA series decreases slightly with the increase of $Ca^{2+}$ which may be due to the increase of $E'$ in rubbery state. For SMP, it shows a higher restoring force with a higher $E'$ in rubbery state, which leads to a higher shrinkage after unloading. Similarly, ODA-BPDA-5 with a lower $E'$ in rubbery state

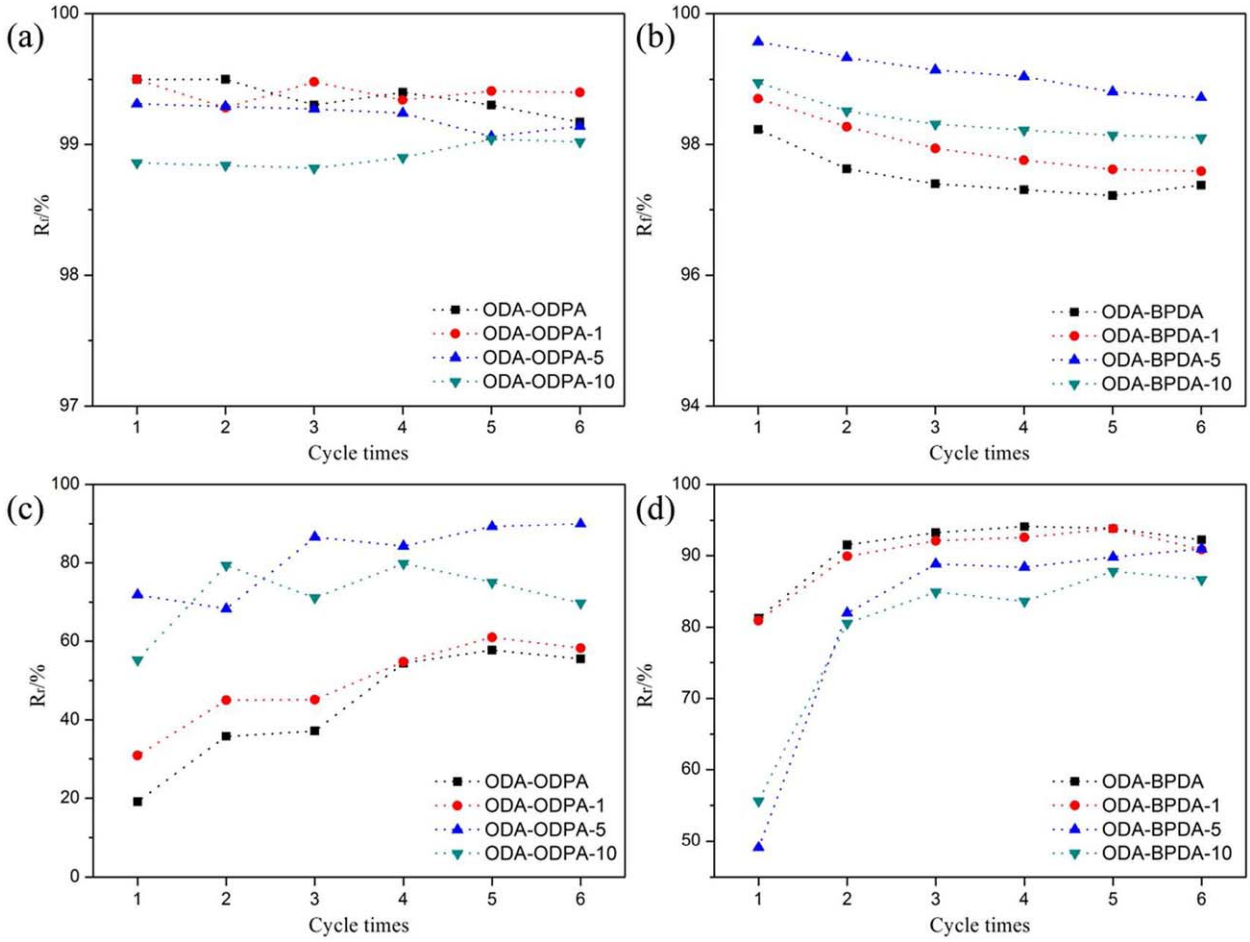


**Figure 8.** Shape memory properties of PI and ionomers during different cycle times: $R_f$ of (a) ODA-ODPA series and (b) ODA-BPDA series; $R_r$ of (a) ODA-ODPA series and (b) ODA-BPDA series. [Color figure can be viewed in the online issue, which is available at wileyonlinelibrary.com.]

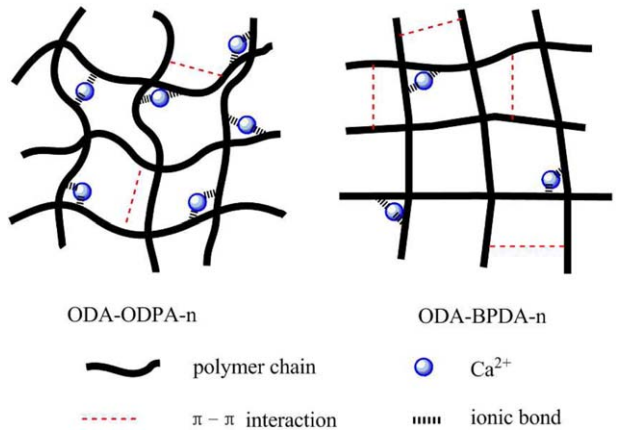


**Figure 9.** Schematic illustration of crosslinked networks for ionomers. [Color figure can be viewed in the online issue, which is available at wileyonlinelibrary.com.]

possesses a higher $R_f$ than other ODA-BPDA based materials, which has been proved in Figure 5. For all that, all polymers show a high $R_f$ over 97%, which is attributed to the massive drop of $E'$ between two states.

As shown in Figure 8(c,d), it is obvious that $R_r$ of PI is affected greatly by the introduction of $Ca^{2+}$ as crosslinked points. First, ODA-ODPA exhibits poor shape recovery performance with only 19.1% for the first cycle and 55.5% for the sixth cycle, while ODA-BPDA shows high shape recover ratio with 81.2% for the first cycle and 92.2% for the sixth cycle. According to the dual-state mechanism of shape memory effect, the fixation of temporary shape depends on the reversible phase while the shape recovery performance is mainly determined by the fixed phase. Therein, the fixed phase could be physical or chemical crosslinked points in the polymer networks. For ODA-BPDA and ODA-ODPA, being a thermoplastic PI, the fixed phase is mainly comprised of physical crosslinked interaction, especially the π-π interaction. In our previous study, it has been proved that ODA-BPDA possessed a stronger π-π interaction with higher chain linearity and rigidity than ODA-ODPA, so ODA-BPDA could show well shape memory performance.[21] Similarly, $R_r$ of PI increases with the increase of cycle times due to the increase of π-π interaction during cycle process. However, the introduction of $Ca^{2+}$ as crosslinked points has opposite effect on the shape recovery performance for ODA-ODPA and ODA-BPDA. The shape recovery performance of ODA-ODPA could be greatly improved with the crosslinked interaction of $Ca^{2+}$: the $R_r$ in the first cycle increases from 19.1% of ODA-ODPA to 71.8% of ODA-ODPA-5, while it increases from 55.5% to 90.0% in the sixth cycle. The significant increase of $R_r$ in the first cycle indicates the obvious function of ionic networks as fixed phase in ODA-ODPA-*n*. For ODA-BPDA, the shape recovery performance decreases after the introduction of $Ca^{2+}$: the $R_r$ in the first cycle decreases from 81.5% of ODA-BPDA to 45.6% of ODA-BPDA-10, while it decreases from 92.2% to 86.7% in the sixth cycle. The high shape recovery performance for ODA-BPDA is ascribed to its strong π-π interaction as fixed phase. Although the introduction of $Ca^{2+}$ could form new ionic crosslinked networks, it also destroys the chain structure of ODA-BPDA, leading to reduction of π-π interaction. For ODA-BPDA series, the strength of increase ionic crosslinked interaction is inferior to the decrease of π-π interaction after ionic crosslinking, so the $R_r$ of ODA-BPDA-*n* decreases after ionic crosslinking. For ODA-ODPA series, the π-π interaction of the original ODA-ODPA is weak, so the increase of ionic crosslinked interaction is more important, resulting in the increase of $R_r$. However, the increase of $R_r$ with the increase of cycle times also indicates the function of π-π interaction as fixed phase. It demonstrates that the fixed phase of inonmers is comprised of two crosslinked interactions: π-π interaction and ionic crosslinked interaction. The structure of crosslinked networks for inomers is manifested in Figure 9. As presented in the schematic diagram, with a flexible chain structure, the π-π interaction of ODA-ODPA-*n* is relatively weak, so the ionic crosslinked interaction plays as the major role of fixed phase for ODA-ODPA-*n*. With high chain rigidity, ODA-BPDA shows a stronger π-π interaction, but it will be weakened due to the introduction of ionic crosslinked interaction. So the fixed phase of ODA-BPDA-*n* is composed of π-π interaction and ionic crosslinked interaction. In conclusion, the introduction of ionic crosslinked networks indeed improves the shape memory properties of PI.

## CONCLUSIONS

A series of PI ionomers with $Ca^{2+}$ crosslinked interaction are prepared in this study. From the results, it is found that the introduction of $Ca^{2+}$ would bring two effects to PI: destructive effect of chain structure and formation of ionic crosslinked interaction. These two effects would exert different influence on ODA-ODPA and ODA-BPDA due to different chain structure. The ionic crosslinked interaction can enhance the mechanical properties, $T_g$, $E'$ at rubbery state of ODA-ODPA while not for ODA-BPDA. The shape recovery performance of ODA-ODPA is also improved because of the increase of ionic crosslinked interaction as fixed phase. For example, the $R_r$ in the first cycle is increased from 19.1% of ODA-ODPA to 71.8% of ODA-ODPA-5, while it increases from 55.5% to 90.0% in the sixth cycle. But for ODA-BPDA-*n*, the shape recovery performance decreases after the introduction of $Ca^{2+}$. Therefore, the mechanical and shape memory properties of ODA-ODPA could be improved by the introduction ionic crosslinked interaction as previous thought. It provides a novel method to enhance the properties of PI, which has great potential in severe conditions, like aerospace industry field.

## ACKNOWLEDGMENTS

The present study was supported by the National Natural Science Foundation of China (No. 11372108), the Natural Science Foundation of Hunan Proince, China (No. 14JJ5021), Open Fund Project Innovation Platform of University in Hunan Province, China (No. 13K098), and High-level talents support plan of Xiamen University of Technology (No. YKJ14035R).

## REFERENCES

1. Lendlein, A.; Kelch, S. *Angew. Chem. Int. Ed.* **2002**, *41*, 2034.
2. Nguyen, T. D.; Yakacki, C. M.; Brahmbhatt, P. D.; Chambers, M. L. *Adv. Mater.* **2010**, *22*, 3411.

3. Leng, J.; Lan, X.; Liu, Y.; Du, S. *Prog. Mater. Sci.* **2011**, *56*, 1077.
4. Behl, M.; Razzaq, M. Y.; Lendlein, A. *Adv. Mater.* **2010**, *22*, 3388.
5. Hu, J.; Zhu, Y.; Huang, H.; Lu, J. *Prog. Polym. Sci.* **2012**, *37*, 1720.
6. Singhal, P.; Small, W.; Cosgriff-Hernandez, E.; Maitland, D. J.; Wilson, T. S. *Acta Biomater.* **2014**, *10*, 67.
7. Huang, W. M.; Song, C. L.; Fu, Y. Q.; Wang, C. C.; Zhao, Y.; Purnawali, H.; Lu, H. B.; Tang, C.; Ding, Z.; Zhang, J. L. *Adv. Drug. Deliver. Rev.* **2013**, *65*, 515.
8. Zhao, J.; Chen, M.; Wang, X.; Zhao, X.; Wang, Z.; Dang, Z. M.; Ma, L.; Hu, G. H.; Chen, F. *ACS Appl. Mater. Inter.* **2013**, *5*, 5550.
9. Fei, P.; Cavicchi, K. A. *ACS Appl. Mater. Inter.* **2010**, *2*, 2797.
10. Zhang, D. W.; Giese, M. L.; Prukop, S. L.; Grunlan, M. A. *J. Polym. Sci. Pol. Chem.* **2011**, *49*, 754.
11. Wang, Z.; Hansen, C.; Ge, Q.; Maruf, S. H.; Ahn, D. U.; Qi, H. J.; Ding, Y. *Adv. Mater.* **2011**, *23*, 3669.
12. Zhang, Y.; Wang, Q.; Wang, C.; Wang, T. *J. Mater. Chem.* **2011**, *21*, 9073.
13. Guo, W.; Lu, C.; Orbach, R.; Wang, F.; Qi, X.; Cecconello, A.; Seliktar, D.; Willner, I. *Adv. Mater.* **2015**, *27*, 73.
14. Zhao, Q.; Behl, M.; Lendlein, A. *Soft Matter.* **2013**, *9*, 1744.
15. Yu, K.; Xie, T.; Leng, J. S.; Ding, Y. F.; Qi, H. J. *Soft Matter* **2012**, *8*, 5687.
16. Voit, W.; Ware, T.; Dasari, R. R.; Smith, P.; Danz, L.; Simon, D.; Barlow, S.; Marder, S. R.; Gall, K. *Adv. Funct. Mater.* **2010**, *20*, 162.
17. Bai, Y.; Jiang, C.; Wang, Q.; Wang, T. *Carbohyd. Polym.* **2013**, *96*, 522.
18. Shi, Y.; Yoonessi, M.; Weiss, R. A. *Macromolecules* **2013**, *46*, 4160.
19. Liu, Y.; Du, H.; Liu, L.; Leng, J. *Smart Mater. Struct.* **2014**, *23*, 023001.
20. Xie, T. *Polymer* **2011**, *52*, 4985.
21. Wang, Q.; Bai, Y.; Chen, Y.; Ju, J.; Zheng, F.; Wang, T. *J. Mater. Chem. A* **2015**, *3*, 352.
22. Yoonessi, M.; Shi, Y.; Scheiman, D. A.; Lebron-Colon, M.; Tigelaar, D. M.; Weiss, R. A.; Meador, M. A. *ACS Nano* **2012**, *6*, 7644.
23. Koerner, H.; Strong, R. J.; Smith, M. L.; Wang, D. H.; Tan, L. S.; Lee, K. M.; White, T. J.; Vaia, R. A. *Polymer* **2013**, *54*, 391.
24. Xiao, X.; Kong, D.; Qiu, X.; Zhang, W.; Zhang, F.; Liu, L.; Liu, Y.; Zhang, S.; Hu, Y.; Leng, J. *Macromolecules* **2015**, *48*, 3582.
25. Liu, J.; Gao, Y.; Wang, F.; Li, D.; Xu, J. *J. Mater. Sci.* **2002**, *37*, 3085.
26. Ragosta, G.; Abbate, M.; Musto, P.; Scarinzi, G. *J. Mater. Sci.* **2012**, *47*, 2637.
27. Sanderson, R. T. Polar Covalence; Academic Press: New York, **1983**.
28. Bratsch, S. G. *J. Chem. Educ.* **1985**, *62*, 101.
29. Burattini, S.; Greenland, B. W.; Hayes, W.; Mackay, M. E.; Rowan, S. J.; Colquhoun, H. M. *Chem. Mater.* **2010**, *23*, 6.
30. He, M.; Zhang, H.; Chen, W. Polymer Physics, 3 ed.; Fudan University: Shanghai, **2013**.
31. Miaudet, P.; Derré, A.; Maugey, M.; Zakri, C.; Piccione, P. M.; Inoubli, R.; Poulin, P. *Science* **2007**, *318*, 1294.